A linear-quadratic unsupervised hyperspectral unmixing method dealing with intra-class variability

Charlotte Revel, Yannick Deville, Véronique Achard, Xavier Briottet

A LINEAR-QUADRATIC UNSUPERVISED HYPERSPECTRAL UNMIXING METHOD DEALING WITH INTRA-CLASS VARIABILITY

Charlotte Revel[1,2], Yannick Deville[1]

[1]Université de Toulouse, UPS-CNRS-OMP
IRAP (Institut de Recherche en Astrophysique et Planétologie)
14 Av. Édouard Belin, F-31400 Toulouse, France

Véronique Achard[2], Xavier Briottet[2]

[2]ONERA "The French Aerospace Lab"
2 Av. Édouard Belin, 31000 Toulouse, France

ABSTRACT

In hyperspectral imagery, unmixing methods are often used to analyse the composition of the pixels. Such methods usually suppose that a unique spectral signature, called an endmember, can be associated with each pure material present in the scene. This assumption is no more valid for materials that exhibit spectral variability due to illumination conditions, weathering, slight variations of the composition, etc. Methods currently appear dealing with this spectral variability and based on linear mixing assumption. However, intra-class variability issues frequently appear in non-flat scenes, and particularly in urban scenes. For urban scenes, the linear-quadratic mixing models better depict the radiative transfer. In this paper, we propose a new unsupervised unmixing method based on the assumption of a linear-quadratic mixing model, that deals with intra-class spectral variability. A new formulation of linear-quadratic mixing is proposed. An unmixing method is presented to process this new model. The method is tested on a semi-synthetic data set built with spectra extracted from a real hyperspectral image and mixtures of these spectra. Based on the results of non-linear and linear unmixing, we discuss the interest of considering the non-linearity regarding the impact of intra-class variability.

Index Terms— Hyperspectral unmixing, linear-quadratic mixing model, intra-class variability, pixel-by-pixel Nonnegative Matrix Factorisation (NMF), real data set.

1. PROBLEM STATEMENT

In the framework of remote sensing, unmixing is a common way to deal with mixed pixels in hyperspectral images. This technique extracts subpixel information in hyperspectral images which are usually less spatially resolved than panchromatic or multispectral images. Unmixing aims at extracting the reflectance spectra of pure materials and the associated proportions in each pixel. An extensive review of unmixing is available in [1]. A common approach of unmixing problems assumes that the spectra in all pixels are linear mixtures of the same pure reflectance spectra. Under this assumption, each observed reflectance spectrum, $\mathbf{x_p} \in \mathbb{R}^{L\times 1}$, can be written as follows:

$$\mathbf{x_p} = \sum_{m=1}^{M} c_{p,m}\mathbf{r_m} \quad \forall p \in \{1,\dots,P\} \tag{1}$$

where p is the pixel index and P the number of pixels, m the index of one of the M pure materials present "in the data", $\mathbf{r_m} \in \mathbb{R}^{L\times 1}$ is the reflectance spectrum of the m^{th} material and $c_{p,m}$ is the associated coefficient. Reflectance spectra and coefficients are assumed to be nonnegative. Besides, the coefficients corresponding to all materials m are most often assumed to sum to one in each pixel p [2]. This sum-to-one condition reads:

$$\sum_{m=1}^{M} c_{p,m} = 1 \quad \forall p \in \{1,\dots,P\}. \tag{2}$$

Let $\mathbf{X} = [\mathbf{x_1},\dots,\mathbf{x_P}]^T$ denote the hyperspectral data matrix, $\mathbf{R} = [\mathbf{r_1},\dots,\mathbf{r_M}]^T$ the pure spectral reflectance matrix and $\mathbf{C} = [\mathbf{c_1},\dots,\mathbf{c_P}]^T$ the coefficient matrix. For each pixel p, $\mathbf{c_p} = [\mathbf{c_{p,1}},\dots,\mathbf{c_{p,M}}]^T$ is an M-dimensional vector, containing the set of coefficients associated with the pixel p. The number of pure spectra, M, is assumed to be known in the rest of the paper. The linear mixing model (1) can then be written as follows:

$$\mathbf{X} = \mathbf{CR}. \tag{3}$$

The above model is based on a strong assumption: a material can be described by a single spectrum. However, in practice, for a same material the spectrum depends on the illumination, its deteriorations, etc [3]. This phenomenon, the so-called intra-class variability, leads one to develop methods able to deal with intra-class variability. In [4], several such methods were detailed. None of them proposes to modify the linear model. In [5], a new linear mixing model was introduced. It assumes that all the spectra that describe a material result from a same spectrum multiplied by a scale factor which differs from a pixel to another. This model assumes that intra-class variability is only due to illumination variations, for instance because of landscape slope variations in non-flat areas. However it does not take into account other types of variability (material wear, composition variation). In [6], another model is introduced aiming to describe more complex intra-class variability structures. Each pure material is no longer described by only one spectrum but by a set of spectra (one per pixel). So the mixing model (1) can be rewritten as:

$$\mathbf{x_p} = \sum_{m=1}^{M} c_{p,m}\mathbf{r_m}(p) \quad \forall p \in \{1,\dots,P\} \tag{4}$$

where $\mathbf{r_m}(p)$ is the reflectance spectrum associated with the material m and the pixel p. The coefficients $c_{p,m}$ still verify the sum-to-one condition (2).

All these models allow one to describe the intra-class variability assuming linear mixing of the spectra. However these variabilities are partly related to the fact that areas are non-flat, and that non-linear effects can appear in these scenes due to multiple scattering. Linear-quadratic model are proposed in [7] and [8]. The model proposed by Meganem et al. was selected since it is based on a specific study of radiative transfers in urban areas, [9]:

This work was funded by the French ANR HYperspectral imagery for Environmental urban Planning (HYEP) project (ANR 14-CE22-0016-01).

$$\mathbf{x_p} = \sum_{m=1}^{M} c_{p,m}\mathbf{r_m} + \sum_{m=1}^{M}\sum_{\mu=m}^{M} c_{p,(m,\mu)}(\mathbf{r_m} \odot \mathbf{r}_\mu), \forall p \quad (5)$$

$$\text{with: } \begin{cases} \sum_{m=1}^{M} c_{p,m} = 1 & (6a) \\ c_{p,m} \geq 0, \qquad m = 1, \cdots, M & (6b) \\ 0 \leq c_{p,(m,\mu)} \leq 0.5, \qquad 1 \leq m \leq \mu \leq M & (6c) \end{cases}$$

where $c_{p,(m,\mu)}$ is the mixing coefficient of the quadratic term obtained by the Hadamard product, $\odot$, between $\mathbf{r_m}$ and $\mathbf{r}_\mu$. Surveys of blind source separation methods applicable to this model are e.g available in [10], [11]. This model does not take into account the intra-class variability. However, we here extend it, as in [6] for linear mixtures, to obtain a new model which assumes that the spectra involved in observed image pixels are independent from one pixel to another. This can be written as follows:

$$\mathbf{x_p} = \sum_{m=1}^{M} c_{p,m}\mathbf{r_m}(p) + \sum_{m=1}^{M}\sum_{\mu=m}^{M} c_{p,(m,\mu)}(\mathbf{r_m}(p) \odot \mathbf{r}_\mu(p)), \forall p, \quad (7)$$

with (6a), (6b) and (6c).

This model allows one to take intra-class variability into account, which is required to achieve accurate unmixing. The method proposed hereafter achieves unmixing based on this new model, introducing both intra-class variability and multiple scattering effects. The Nonnegative Matrix Factorisation [12] is extended and constrained to solve (7) under (6a), (6b) and (6c). Sec. 2 overviews the proposed linear-quadratic method. Sec. 3 presents experimental results. The relevance of introducing quadratic terms in the model is discussed. The conclusions are given in Sec. 4.

2. UNMIXING METHOD

To obtain a matrix expression for the model (7), let $\mathbf{R}(p) = [\mathbf{r_1}(p), \ldots, \mathbf{r_M}(p)]^T$ and $\mathbf{T}(p) = [\mathbf{r_1}(p) \odot \mathbf{r_1}(p), \mathbf{r_1}(p) \odot \mathbf{r_2}(p), \ldots, \mathbf{r_M}(p) \odot \mathbf{r_M}(p)]^T$ respectively be the set of M constituent material spectra and the set of $K = M^2 - \binom{M}{2}$ "quadratic spectra" associated with the pixel p, $\tilde{\mathbf{R}} = \begin{bmatrix} \mathbf{R}(1) \\ \vdots \\ \mathbf{R}(P) \end{bmatrix}$, and $\tilde{\mathbf{T}} = \begin{bmatrix} \mathbf{T}(1) \\ \vdots \\ \mathbf{T}(P) \end{bmatrix}$ respectively the matrices containing all the pure spectra and all the quadratic spectra. $\gamma_\mathbf{p} = [c_{p,(11)}, c_{p,(12)}, \ldots, c_{p,(MM)}]^T$ is a K-dimensional vector, containing the set of "quadratic coefficients" associated with the pixel p. Then Eq. (7) may be rewritten as follows:

$$\mathbf{x_p}^T = \mathbf{c_p}^T\mathbf{R}(p) + \gamma_\mathbf{p}{}^T\mathbf{T}(p). \quad (8)$$

Let $\tilde{\mathbf{C}} \in \mathbb{R}^{P \times PM}$ and $\tilde{\mathbf{\Gamma}} \in \mathbb{R}^{P \times PK}$ be block-diagonal matrices, denoting the new coefficient matrices:

$$\tilde{\mathbf{C}} = \begin{bmatrix} \mathbf{c_1}^T & 0\ldots0 & \ldots & 0\ldots0 \\ 0\ldots0 & \mathbf{c_2}^T & \ldots & 0\ldots0 \\ & & \ddots & \\ 0\ldots0 & 0\ldots0 & \ldots & \mathbf{c_P}^T. \end{bmatrix} \quad (9)$$

$$\tilde{\mathbf{\Gamma}} = \begin{bmatrix} \gamma_\mathbf{1}{}^T & 0\ldots0 & \ldots & 0\ldots0 \\ 0\ldots0 & \gamma_\mathbf{2}{}^T & \ldots & 0\ldots0 \\ & & \ddots & \\ 0\ldots0 & 0\ldots0 & \ldots & \gamma_\mathbf{P}{}^T \end{bmatrix} \quad (10)$$

Then, based on the mixing model described in Eq. (7), the data matrix $\mathbf{X} = [\mathbf{x_1}, \ldots, \mathbf{x_P}]^T$ can be written as:

$$\mathbf{X} = \tilde{\mathbf{C}}\tilde{\mathbf{R}} + \tilde{\mathbf{\Gamma}}\tilde{\mathbf{T}}. \quad (11)$$

It is possible to reduce Eq. (11) to an expression similar to the linear model (3). Let $\dot{\mathbf{R}}$ be the matrix containing all the pure spectra and all the "quadratic spectra", $\dot{\mathbf{R}} = \begin{bmatrix} \mathbf{R}(1) \\ \mathbf{T}(1) \\ \vdots \\ \mathbf{R}(P) \\ \mathbf{T}(P) \end{bmatrix}$. The coefficient matrix associated with $\dot{\mathbf{R}}$ is called $\dot{\mathbf{C}} \in \mathbb{R}^{P \times P(M+K)}$ and can be written as follows:

$$\dot{\mathbf{C}} = \begin{bmatrix} [\mathbf{c_1}^T, \gamma_\mathbf{1}{}^T] & 0\ldots0 & \ldots & 0\ldots0 \\ 0\ldots0 & [\mathbf{c_2}^T, \gamma_\mathbf{2}{}^T] & \ldots & 0\ldots0 \\ & & \ddots & \\ 0\ldots0 & 0\ldots0 & \ldots & [\mathbf{c_P}^T, \gamma_\mathbf{P}{}^T]. \end{bmatrix} \quad (12)$$

So, Eq. (11) yields the matrix form of the mixing model in Eq. (7):

$$\mathbf{X} = \dot{\mathbf{C}}\dot{\mathbf{R}}. \quad (13)$$

In the unmixing method hereafter developed, the constraints (6a) to (6c) on $\mathbf{c_p}$ (or $\tilde{\mathbf{C}}$) and $\gamma_\mathbf{p}$ (or $\tilde{\mathbf{\Gamma}}$) are enforced after each update. Even with these constraints, Eq. (13) yields a Nonnegative Matrix Factorisation non-convex problem.

2.1. Inertia-constrained Pixel-by-pixel NMF (IP-NMF)

In [6], we developed an unmixing method, called IP-NMF, dealing with (4). IP-NMF is a method inspired from Lin's standard Nonnegative Matrix Factorisation algorithm [13]. It aims at decomposing each observed spectrum into pure spectra which are specific to the considered pixel. To constrain the spectra search, an inertia constraint is introduced. This leads one to minimise the following cost function:

$$J_{IPNMF} = \frac{1}{2}\|\mathbf{X} - \tilde{\mathbf{C}}\tilde{\mathbf{R}}\|_F^2 + \mu\sum_{m=1}^{M} Tr(Cov(\mathbf{R}_{\mathcal{C}_m})) \quad (14)$$

where $\tilde{\mathbf{C}}$, $\tilde{\mathbf{R}}$ and $\mathbf{R}_{\mathcal{C}_m}$ are *estimated* variables, $\mathbf{R}_{\mathcal{C}_m} \in \mathbb{R}^{P \times L}$ denotes the set of reflectance spectra of the m^{th} pure material extracted in the P pixels, μ the constraint parameter and $Tr(Cov(\mathbf{R}_{\mathcal{C}_m}))$ the trace of the $\mathbf{R}_{\mathcal{C}_m}$ covariance matrix (or inertia of the m^{th} class of materials). An expression of the resulting update algorithm is given in [6]. We hereafter show how to extend IP-NMF to solve our linear-quadratic unmixing problem.

2.2. Linear-Quadratic Inertia-constrained Pixel-by-pixel NMF (LQIP-NMF)

The linear-quadratic mixing model we defined, introduced a sum of quadratic terms in addition to the linear model considered in IP-NMF. In our extended IP-NMF cost function, this term has to be taken into account. It is introduced in the reconstruction error term, $J_{RE} = \frac{1}{2}\|\mathbf{X} - (\tilde{\mathbf{C}}\tilde{\mathbf{R}} + \tilde{\mathbf{\Gamma}}\tilde{\mathbf{T}})\|_F^2$. The inertia constraint remains the same. The overall cost function to be minimised becomes:

$$J_{quad} = \frac{1}{2}\|\mathbf{X} - \dot{\mathbf{C}}\dot{\mathbf{R}}\|_F^2 + \mu\sum_{m=1}^{M} Tr(Cov(\mathbf{R}_{\mathcal{C}_m})). \quad (15)$$

The choice of notations yields a quite simple expression for J_{quad}. However, due to the quadratic terms, the associated update algorithm cannot be written as simply. Our calculations of the gradients show that the resulting bare update of LQIP-NMF, i.e. before enforcing (6a) to (6c) and zero forcing in $\dot{\mathbf{C}}$, is:

$$\dot{\mathbf{C}} \longleftarrow \dot{\mathbf{C}} + \alpha_{\dot{C}}.(\mathbf{X} - \dot{\mathbf{C}}\dot{\mathbf{R}})\dot{\mathbf{R}}^T$$

$$[\tilde{\mathbf{R}}]_{\nu l} \longleftarrow \{[\tilde{\mathbf{R}}]_{\nu l} + \alpha_{\dot{R}}.([\tilde{\mathbf{C}}^T(\mathbf{X} - \dot{\mathbf{C}}\dot{\mathbf{R}})]_{\nu l} + \sum_{\substack{\mu=(p-1)M+1 \\ \mu\neq\nu}}^{pM} [\tilde{\mathbf{R}}]_{\mu l} \times [\tilde{\mathbf{\Gamma}}^T(\mathbf{X} - \dot{\mathbf{C}}\dot{\mathbf{R}})]_{(\mu\nu)l}$$

$$+ 2[\tilde{\mathbf{R}}]_{\nu l} \times [\tilde{\mathbf{\Gamma}}^T(\mathbf{X} - \dot{\mathbf{C}}\dot{\mathbf{R}})]_{(\nu\nu)l} - \frac{2\mu}{P} \times [\mathbf{Id}_{PM} - \frac{1}{P}\mathbf{U})\tilde{\mathbf{R}}]_{\nu l})\}$$

$$[\tilde{\mathbf{T}}]_{(\mu m)l} \longleftarrow [\tilde{\mathbf{R}}]_{\mu l} \times [\tilde{\mathbf{R}}]_{ml}$$

where ν is the row index in $\tilde{\mathbf{R}}$ which corresponds to material m in pixel p, (μm) is the index of the matrix $\tilde{\mathbf{T}}$ row, respectively $\tilde{\mathbf{\Gamma}}$ column, corresponding to the "quadratic spectrum" $[\tilde{\mathbf{R}}]_{\mu\cdot} \odot [\tilde{\mathbf{R}}]_{m\cdot}$ for pixel p, respectively the coefficient $c_{p,(\mu m)}$, and with $\mathbf{Id}_{PM}$ the identity matrix of size PM and $\mathbf{U} \in \mathbb{R}^{PM\times PM}$ the "spectrum selection" matrix:

$$\mathbf{U} = \mathbb{1}_{PP} \otimes \mathbf{Id}_M$$

where $\otimes$ is the Kronecker product symbol. We hereafter propose a computationally more efficient matrix form for the above update. It assumes that the "quadratic elements" (spectra and coefficients) are organised as follows: $\gamma_p = [c_{p,(11)}, \cdots, c_{p,(1M)}, c_{p,(22)}, \cdots, c_{p,(MM)}]^T = [c_{p,(\mu\nu)}]_{\substack{1\leqslant\mu\leqslant M \\ \mu\leqslant\nu\leqslant M}}^{T}$. The bare update becomes:

$$\dot{\mathbf{C}} \longleftarrow \dot{\mathbf{C}} + \alpha_{\dot{C}}.(\mathbf{X} - \dot{\mathbf{C}}\dot{\mathbf{R}})\dot{\mathbf{R}}^T$$

$$\tilde{\mathbf{R}} \longleftarrow \{\tilde{\mathbf{R}} + \alpha_{\tilde{R}}.(\tilde{\mathbf{C}}^T(\mathbf{X} - \dot{\mathbf{C}}\dot{\mathbf{R}}) - \frac{2\mu}{P} \times (\mathbf{Id}_{PM} - \frac{1}{P}\mathbf{U})\tilde{\mathbf{R}}$$
$$+ ((\mathbf{Id}_{PM} \otimes \mathbb{1}_{1K})(((\mathbf{Id}_P \otimes \mathbf{F})(\mathbf{Id}_P \otimes (\mathbb{1}_{M1} \otimes \mathbf{Id}_M))\tilde{\mathbf{R}})$$
$$\odot ((\mathbf{Id}_P \otimes (\mathbb{1}_{M1} \otimes \mathbf{Id}_K))\tilde{\mathbf{\Gamma}}(\mathbf{X} - \dot{\mathbf{C}}\dot{\mathbf{R}})))))\}$$

$$\tilde{\mathbf{T}} \longleftarrow \big((\mathbf{Id}_P \otimes \mathbf{G_1})\tilde{\mathbf{R}}\big) \odot \big((\mathbf{Id}_P \otimes \mathbf{G_2})\tilde{\mathbf{R}}\big)$$

where $\mathbf{G_1} \in \mathbb{R}^{K\times M}$ and $\mathbf{G_2} \in \mathbb{R}^{K\times M}$ are two selection matrices and $\mathbf{F} \in \mathbb{R}^{MK\times M^2}$ is a block-diagonal selection matrix such that:

$$[\mathbf{G_1}]_{km} = \sum_{\alpha=1}^{M}\sum_{\beta\geqslant\alpha}^{M} \delta^k_{(\alpha-1)(M-\frac{\alpha}{2})+\beta}.\delta^\alpha_m$$

$$[\mathbf{G_2}]_{km} = \sum_{\alpha=1}^{M}\sum_{\beta\geqslant\alpha}^{M} \delta^k_{(\alpha-1)(M-\frac{\alpha}{2})+\beta}.\delta^\beta_m$$

$$\mathbf{F} = \begin{bmatrix} \mathbf{F_1} & \cdots & (\mathbf{0}) \\ \vdots & \ddots & \vdots \\ (\mathbf{0}) & \cdots & \mathbf{F_M} \end{bmatrix}$$

$$[\mathbf{F}_\mu]_{km} = \sum_{\nu=1}^{M} \delta^\nu_m \delta^\eta_k (1 + \delta^\mu_\nu)$$

$$\eta = (min(\mu,\nu) - 1)(M - \frac{min(\mu,\nu)}{2}) + max(\mu,\nu)$$

where δ^j_i is the Kronecker symbol. If a different organization of the "quadratic elements" is used, only $\mathbf{F}$ has to be adapted in the update rules.

3. TEST RESULTS

3.1. Test description

The spectra used to perform the tests were extracted from a hyperspectral image taken above Toulouse, France. Toulouse city is composed of a large number of characteristic urban areas. Its downtown is typical from old cities in the South of France: tile roofs, low rise homes or big architectural monuments (cathedral, town hall...), green spaces (public gardens, squares...),... Due to its 1.8 m resolution, this image contains many pure spectra. Hence we were able to extract a large number of spectra to take into account various phenomena responsible for intra-class variability: illumination variation, various material weatherings... The tested data are semi-synthetic. The pure spectra (hereafter called reference spectra) used to create the mixed data are extracted from the above urban area image. They thus describe realistic intra-class variabilities. Tests were performed on an image containing 21 squares of 6×6 pixels. In each square, all mixing coefficients were fixed (cf. Fig. 1) and $M = 3$ reference spectra in each pixel were randomly extracted from 3 sets of spectra (tiles, vegetation and asphalt) built from the image. The 3 linear abundance maps corresponding to this first tested scenario are shown in the first column of Fig. 1. A quadratic term is added to linear terms in some squares while respecting the model (7). We fixed this term to 0.3 according to [14] and to have a significant quadratic coefficient. This term is added in the squares of the last 3 columns of the reference abundance maps of the 1^{st} column of Fig. 1, as shown in the first column of Fig. 2. The proposed method needs an initialisation. Using the results in [6], the linear spectra were initialised with the result of a standard unmixing method, VCA [15] + FCLS, and the linear coefficients, respectively the quadratic ones, were initialised to $\frac{1}{M}$, respectively to 0.2.

3.2. Performance criteria

A major point to be evaluated is the differences between estimated pure material reflectance spectra and reference spectra really present in the pixels. To this end we computed, in each pixel, the spectral angles (SAM) between these two sets of spectra. Two other criteria were also computed. The first one is the reconstruction error (RE), that shows the effects of our method on the global reconstruction of the image. The second one is the mean square error computed on the linear coefficients (CE).

3.3. Results

To analyse the results, 3 unmixing methods were tested: VCA + FCLS, IP-NMF and LQIP-NMF. In Table 1, the values of all the criteria detailed in Sec. 3.2 are reported. This table shows that IP-NMF yields the best results in this first scenario, followed by LQIP-NMF and VCA + FCLS. To study the impact of the 3 methods pixel by pixel, abundance maps are shown in Fig. 1 and Fig. 2. In Fig. 1, the linear terms are depicted, in Fig. 2 the quadratic terms are shown.

	VCA + FCLS	IP-NMF	LQIP-NMF
SAM ($^\circ$)	9.33	6.46	7.46
RE	8.6	0.28	7.4
CE	2.9	2.9	2.9

Table 1. Results of various unmixing methods.

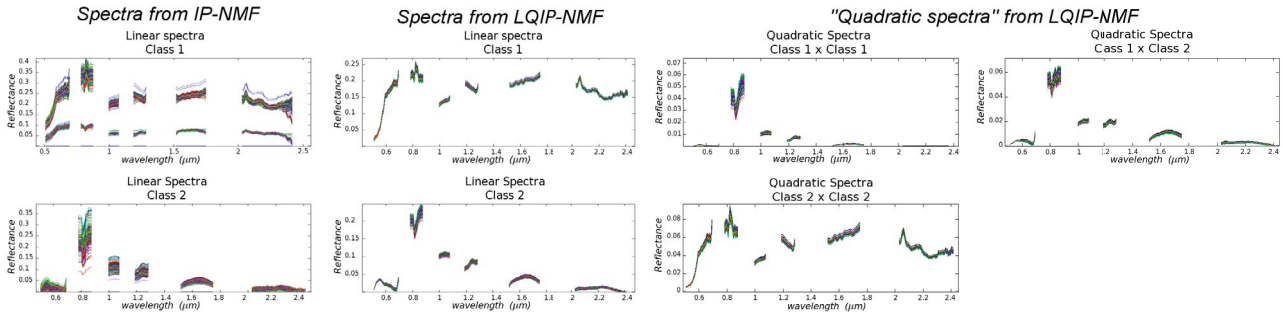

Fig. 3. Spectra and spectra products of 2 classes (tiles (1^{st} row) and vegetation (2^{nd} row)) estimated by IP-NMF (1^{st} column) and LQIP-NMF (2^{nd} to 4^{th} columns) showing the intra-class variability obtained with each method.

As compared with the VCA+FCLS method, IP-NMF and LQIP-NMF linear abundance maps are closer to the reference ones. Indeed less false detections (higher abundances for wrong classes) are observed in Fig. 1 for the latter methods. It is particularly the case for the 3^{rd} class. Visual differences are small between IP-NMF and LQIP-NMF. The quadratic terms cannot be extracted with VCA and IP-NMF but these methods yield well estimated linear terms despite the presence of quadratic terms. The quadratic coefficients obtained by LQIP-NMF are depicted in Fig. 2. The non-zero coefficients are not located as we would hope (last two columns). This phenomenon may be explained as follows. In the first tested scenario, the quadratic mixing coefficients yield low-magnitude terms as compared with the intra-class spectral variability. They are therefore poorly estimated by LQIP-NMF, whose additional variables thus degrade performance. For instance, the intra-class variability for LQIP-NMF spectra is very low compared with the IP-NMF spectra (cf. Fig. 3) and "true" intra-class variability (similar to IP-NMF spectra). In LQIP-NMF, this variability is replaced by the quadratic spectra which are used to reduce the reconstruction error. This explains the location of the quadratic terms in Fig. 2. To show the relevance of this explanation, two methods are used hereafter to modify the above ratio between quadratic terms and spectral variability. The first test consists in increasing the amplitude of the quadratic coefficients. In this case, LQIP-NMF outperforms IP-NMF. For instance, the LQIP-NMF value of the SAM is equal to 6.4° and the IP-NMF value is equal to 7.2°. The second method consists in reducing the intra-class variability. Also in this case, LQIP-NMF outperforms IP-NMF, the SAM value drops from 3.8° with IP-NMF to 2.5° with LQIP-NMF. In both cases, LQIP-NMF improves the results of the unmixing.

4. CONCLUSION

We have developed a new unsupervised hyperspectral unmixing method to address intra-class variability in the linear-quadratic mixing model. This investigation is a first step in the development of a more robust method. Indeed, the small values of coefficients associated with the quadratic spectra and the low amplitude of those spectra limit performance. The amplitude of the variations in a class of materials is higher than the amplitude of estimated quadratic terms. In urban areas the quadratic terms are drowned in the large variability of materials. In this case we can wonder if the quadratic mixture model is relevant. The method was tested in various other cases, in particular with a lower intra-class variability, and then outperformed other methods. So, considering both intra-class variability and non-linear mixing models is very hard. Current work aims at studying the limits of applicability of LQIP-NMF both in terms of amplitude of intra-class variability and studied area. Then we will be able to satisfactorily carry out LQIP-NMF on adapted areas of real images.

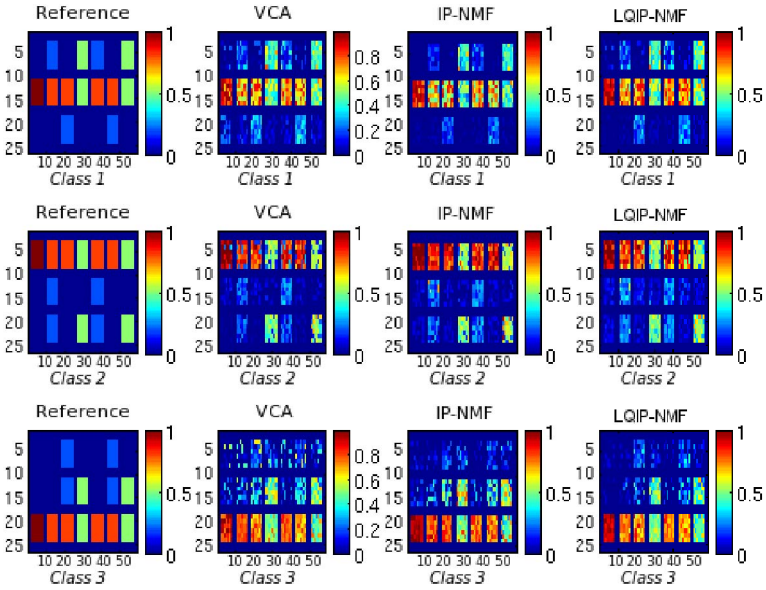

Fig. 1. Reference abundance maps of the linear coefficients of the first scenario (1^{st} column). Abundance maps of the linear coefficients estimated by VCA+FCLS (2^{nd} column), IP-NMF (3^{rd} column), LQIP-NMF (4^{th} column).

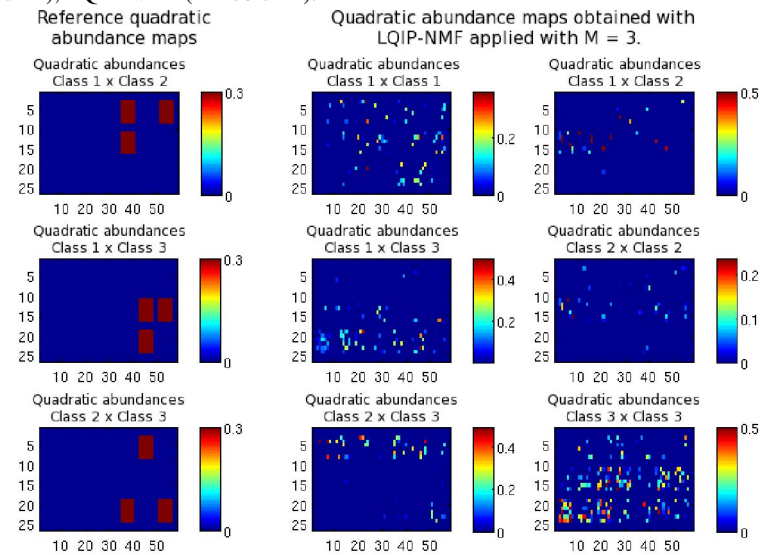

Fig. 2. Abundance maps of the quadratic coefficients: reference (1^{st} column) and maps estimated by LQIP-NMF (2^{nd} - 3^{rd} columns).

5. REFERENCES

[1] J.M. Bioucas-Dias, A. Plaza, N. Dobigeon, M. Parente, Qian Du, P. Gader, and J. Chanussot, "Hyperspectral Unmixing Overview: Geometrical, Statistical, and Sparse Regression-Based Approaches," *IEEE Journal of Selected Topics in Applied Earth Observations and Remote Sensing*, vol. 5, no. 2, pp. 354–379, Apr. 2012.

[2] Nirmal Keshava, "A survey of spectral unmixing algorithms," *Lincoln Laboratory Journal*, vol. 14, no. 1, pp. 55 – 78, 2003.

[3] S. Lacherade, C. Miesch, X. Briottet, and H. Le Men, "Spectral variability and bidirectional reflectance behaviour of urban materials at a 20 cm spatial resolution in the visible and near-infrared wavelengths. A case study over Toulouse (France)," *International Journal of Remote Sensing*, vol. 26, no. 17, pp. 3859–3866, Sept. 2005.

[4] A. Zare and K.C. Ho, "Endmember variability in hyperspectral analysis: Addressing spectral variability during spectral unmixing," *IEEE Signal Processing Magazine*, vol. 31, no. 1, pp. 95–104, Jan. 2014.

[5] M.A. Veganzones, L. Drumetz, G. Tochon, M. Dalla Mura, A. Plaza, J. Bioucas-Dias, and J. Chanussot, "A new extended linear mixing model to address spectral variability," in *2014 6th Workshop on Hyperspectral Image and Signal Processing (WHISPERS)*, Lausanne, Switzerland, June 2014.

[6] C. Revel, Y. Deville, V. Achard, and X. Briottet, "A method based on nonnegative matrix factorization dealing with intra-class variability for unsupervised hyperspectral unmixing," in *2015 7th Workshop on Hyperspectral Image and Signal Processing (WHISPERS)*, Tokyo, Japan, June 2015.

[7] I. Meganem, P. Deliot, X. Briottet, Y. Deville, and S. Hosseini, "Linear quadratic mixing model for reflectances in urban environments," *IEEE Transactions on Geoscience and Remote Sensing*, vol. 52, no. 1, pp. 544–558, Jan. 2014.

[8] Wenyi Fan, Baoxin Hu, John Miller, and Mingze Li, "Comparative study between a new nonlinear model and common linear model for analysing laboratory simulatedforest hyperspectral data," *International Journal of Remote Sensing*, vol. 30, no. 11, pp. 2951–2962, June 2009.

[9] Ines Meganem, *Methodes de separation aveugle de sources pour l'imagerie hyperspectrale : application la teledetection urbaine et l'astrophysique*, Ph.d, Universite de Toulouse, Universite Toulouse III - Paul Sabatier, Dec. 2012.

[10] Yannick Deville and Leonardo Tomazeli Duarte, "An Overview of Blind Source Separation Methods for Linear-Quadratic and Post-nonlinear Mixtures," in *12th International Conference on Latent Variable Analysis and Signal Separation (LVA/ICA 2015)*, Liberec, Czech Republic, Aug. 2015, number 9237, pp. 155–167, Springer International Publishing.

[11] Yannick Deville, "Blind Source Separation and Blind Mixture Identification Methods," in *Wiley Encyclopedia of Electrical and Electronics Engineering*. John Wiley & Sons, Inc., 2016.

[12] Daniel D. Lee and H. Sebastian Seung, "Learning the parts of objects by non-negative matrix factorization," *Nature*, vol. 401, no. 6755, pp. 788–791, Oct. 1999.

[13] Chih-Jen Lin, "Projected gradient methods for nonnegative matrix factorization," *Neural Computation*, vol. 19, no. 10, pp. 2756–2779, 2007.

[14] I. Meganem, Y. Deville, S. Hosseini, P. Deliot, and X. Briottet, "Linear-Quadratic Blind Source Separation Using NMF to Unmix Urban Hyperspectral Images," *IEEE Transactions on Signal Processing*, vol. 62, no. 7, pp. 1822–1833, Apr. 2014.

[15] J.M.P. Nascimento and J.M. Bioucas Dias, "Vertex component analysis: a fast algorithm to unmix hyperspectral data," *IEEE Transactions on Geoscience and Remote Sensing*, vol. 43, no. 4, pp. 898–910, Apr. 2005.